

ALEXANDER POLYNOMIAL OF RIBBON KNOTS AND VIRTUAL KNOTS

SHENG BAI

ABSTRACT. We find that Alexander polynomial of a ribbon knot in $\mathbb{Z}HS^3$ is determined by the intrinsic singularity information of its ribbon, and give a formula to calculate Alexander polynomial of a ribbon knot by that. We define half Alexander polynomial $A_R(t)$, an invariant of oriented ribbons, and in fact the Alexander polynomial of the ribbon knot is $A_R(t)A_R(t^{-1})$. We give two useful simplified formulas for half Alexander polynomial. We characterize completely the polynomials arising as half Alexander polynomials of ribbons. The above study unexpectedly leads us to discover new formulas for Alexander polynomial of general knots and virtual knots in terms of Gauss diagrams.

CONTENTS

1. Introduction	2
1.1. Alexander polynomial of ribbon knots in $\mathbb{Z}HS^3$	2
1.2. Alexander polynomial of general knots and virtual knots	4
2. Background	5
2.1. Alexander polynomials in $\mathbb{Z}HS^3$	5
2.2. Alexander polynomial of virtual knots	5
3. Alexander module of ribbon knots in $\mathbb{Z}HS^3$	6
3.1. Ribbon diagram and ribbon graph	6
3.2. Half Alexander polynomial and the main theorem	6
3.3. Proof of Theorem 3.2.2	8
3.4. Alexander Invariants of ribbon knots	11
4. Half Alexander polynomials of ribbons.	12
4.1. Example: $\Delta_{K_1}(t) = \Delta_{K_2}(t)$ but $A_{R_1}(t) \neq A_{R_2}(t)$.	12
4.2. Topological meaning of half Alexander polynomials.	13
4.3. Reductions	13
4.4. Contracted ribbon graph and contracted formula	15
4.5. Path-type simplified formula	18
4.6. Half Alexander polynomial is not a ribbon knot invariant	21
5. Alexander polynomial of general knots and virtual knots	22
5.1. Motivation: Similarity between ribbon graph and Gauss diagram	22
5.2. New Formulas for classical knots	22
5.3. New formula and contracted formula for virtual knots	28
6. Questions and A Generalization	28

Date: 2023 Jan.18.

2020 Mathematics Subject Classification. 57K10.

Key words and phrases. ribbon knots, Alexander polynomial, Conway polynomial, Fox-Milnor Theorem, Gauss diagram, ribbon number, symmetric union, Fox free differential, Wirtinger representation, virtual knots, integer homology sphere.

6.1. Questions	28
6.2. A generalization	29
References	31

1. INTRODUCTION

Alexander polynomial is one of the most famous and fundamental invariants of knots. There are many methods for computing Alexander polynomial. For example, construct a Seifert surface, choose a homological basis on it and calculate its Seifert matrix. The Alexander polynomial is also computed from a presentation of the knot group, the fundamental group of the knot complements. Thus one can compute the Alexander polynomial of a knot from its diagram, since there are many ways to get a presentation of the knot group from its diagram, like the Wirtinger presentation.

Ribbon knots are slice knots that are easy to describe in R^3 , and Fox conjectured that all slice knots are ribbon knots. We give here a general definition of a ribbon knot.

Definition 1.0.1. Let $r : D^2 \rightarrow M^3$ be a smooth immersion of an oriented disk into a smooth 3-manifold. If each component of the singularities of $r(D^2)$ is an arc and one component of its preimage in D^2 is interior, then $r(\partial D^2)$ is a *ribbon knot*, and $R = r(D^2)$ is a *ribbon*.

A classical result proved by Fox and Milnor[4] is that the Alexander polynomial of a slice knot has the form $f(t)f(t^{-1})$ for some integer-coefficient polynomial $f(t)$. For ribbon knots, we know that we can give a simpler proof of this result in S^3 [10]. Further, a folklore result is that $f(t)$ can be taken to be the Alexander polynomial of the ribbon in B^4 .

There were some fine researches on Alexander polynomials for some special types of ribbon knots, especially symmetric unions and simple-ribbon knots. Symmetric unions were first introduced by Kinoshita and Terasaka[9] in 1957 and generalized by Lamm[11] in 2000. Lamm obtained many properties of Alexander polynomials of symmetric unions [11]. But no one has given a general formula for Alexander polynomials of symmetric unions. Recently, some researchers (c.f.[8]) defined a special class of ribbon knots in technical terms, called simple-ribbon knots, gave a general formula for their Alexander polynomials, and applied their formula to consider some specific problems.

In this paper, we consider general ribbon knots, give general formulas for their Alexander polynomials, and study their properties and variants in details. Furthermore, we always study Alexander polynomial of ribbon knots in a more general setting, i.e., in integer homology spheres.

1.1. Alexander polynomial of ribbon knots in $\mathbb{Z}HS^3$. We will first give a natural definition to record the intrinsic singularity information of an arbitrary ribbon R , called *ribbon diagram*. See Definition 3.1.1. We will then define *ribbon graph* to record the main informations of the ribbon diagram. See Definition 3.1.2. We stress here that ribbon graph is not a graph but a pair consisting of a directed tree and a map from its edges to its vertices. We will define a definite integer-coefficient polynomial called *half Alexander polynomial*, denoted $A_R(t)$, which is determined by the ribbon graph. See Subsection 3.2. Our basic theorem is

Theorem 1.1.1. *Given a ribbon R for a ribbon knot K in $\mathbb{Z}HS^3$, let $A_R(t)$ be the half Alexander polynomial determined by the ribbon graph. Then the Conway-normalized Alexander polynomial of K is $\Delta(t) = A_R(t)A_R(t^{-1})$. Especially, Alexander polynomial of a ribbon knot is determined by its ribbon diagram.*

We emphasize that, unless the ribbon diagram is rather trivial, each ribbon diagram corresponds to infinitely many different ribbons and thus to infinitely many different ribbon knots. Combining more analysis on half Alexander polynomial and ribbon graph, we get a nontrivial upper bound of the breath of Alexander polynomial of a ribbon knot in Corollary 4.3.3.

For the ribbon knots in S^3 , the last statement of Theorem 1.1.1 has long been derived implicitly by some literatures, e.g. [15]. However, the methods in these literatures essentially calculated the fundamental group by diagrams, having nothing to do with Seifert surfaces, so are not valid for ribbon knots in $\mathbb{Z}HS^3$. And the formula for half Alexander polynomial we give in Subsection 3.2, to the best of our knowledge, does not appear in the literature. Even when used in the very specific case of a simple-ribbon knot, it is not directly any formula given by the authors of [8]. For the general procedure we give for computing the Alexander polynomial of ribbon knots, see Subsection 4.3.1.

As a direct corollary of Theorem 1.1.1, we obtain a result on the determinant of a ribbon knot, i.e., Corollary 3.2.4, which generalizes Theorem 2 in [11] of Lamm on the determinant of a symmetric union.

The middle part of this paper examines in depth the half Alexander polynomials in several ways. First, we give a three dimensional topological explanation of half Alexander polynomial in Proposition 4.2.1, different from the previously mentioned folklore one. We also point out with examples that the half Alexander polynomial gives substantially more information about a ribbon than the Alexander polynomial, see Subsection 4.1. More importantly, we point out by counterexamples that the half-Alexander polynomial is not an invariant of ribbon knot, even up to multiplication by $\pm t^{\pm n}$ and changing t by t^{-1} . This has the following implication. In the classical result of Fox and Milnor[4], while they did not say that $f(t)$ is an invariant of the slice knot, they did not deny the possibility either. While it is certainly possible to have different $f(t)$ when the factorization of the Alexander polynomial is not unique, is it possible that there exists a special factorization such that $f(t)$ is somehow indeed an invariant of slice knot? To the best of our knowledge, no literature has explicitly rejected this possibility. And our counterexample illustrates that this is essentially impossible.

The main result of the middle part of our paper is to give two simplified formulas for computing the half Alexander polynomials which are applicable for all cases, they are the *contracted formula* (Theorem 4.4.2) and the *path-type simplified formula* (Theorem 4.5.2). The equivalences of both formulas and the original formula given in Subsection 3.2 are not obvious. They each can greatly simplify the computational effort in some common cases. The path-type formula, although applicable only to the case where the ribbon tree is a path, is also general, since each ribbon can be deformed into this case while keeping the knot type unchanged (Proposition 4.5.1).

Using the path-type simplified formula, we revisit a result of Terasaka[15] that given any integer-coefficient polynomial $f(t)$ satisfying $f(1) = \pm 1$, there exists a ribbon knot whose Alexander polynomial is $f(t)f(t^{-1})$. Note that since the

factorization of an Alexander polynomial may not be unique, logically it does not imply the following result.

Corollary 1.1.2. *Given a polynomial $f(t)$ with integer coefficients and $f(1) = \pm 1$, there is a ribbon with fusion number 1 so that the half Alexander polynomial $A_R(t) = f(t)$.*

However, if we examine Terasaka's construction [15], we find that his construction already satisfies the above result. We prove the above result using the path-type simplified formula, and our construction is much more compact and regular.

At the end of the paper, we will give a generalization of our main theorem and main formula, namely Theorem 6.2.1, which gives a formula for the Alexander polynomial for the band sum of knots. Although this seems to be of little theoretical significance, it has received a lot of attention. In fact, the whole paper [15] is about computing the Alexander polynomial for the band sum of a knot and an unknot using the Wirtinger representation, while the main point of paper [8] is to compute the Alexander polynomial for a very special band sum of a knot and many unknots. The method of paper [8] also uses Seifert surfaces, but it uses a variety of special techniques such as sliding, winding and tubing, while ours is relatively uniform and general.

1.2. Alexander polynomial of general knots and virtual knots. Applying our formula in Section 3.2 to a special type of ribbon knot, the connected sum of a knot and its mirror image, unexpectedly inspires us to discover a new formula for computing the Alexander polynomial for a general knot. The application of our formulas to virtual knots sometimes simplifies the calculation even more.

Gauss diagram is a way to represent a knot. Actually, the Gauss diagram represents more general object called virtual knots, and not all the Gauss diagrams represent a knot. Thus it is an interesting problem to explore a Gauss diagram formula for knot invariants, because such a formula may bring an extension of a knot invariant to a virtual knot invariant.

Although Alexander polynomial is a quite classical invariant, looking for new algorithmic formula for Alexander polynomial is still attracting for some knot theorists in these decades. In the spirit of [6] that any finite type invariant of knots can be computed from a Gauss diagram, by counting suitable sub-Gauss diagrams, in [2], the authors gave an explicit Gauss diagram formula for the coefficients of Conway polynomial. Their proof was purely combinatorial, by induction on the number of crossings.

We give a formula for the whole Alexander polynomial in terms of Gauss diagram, which is quite different from the formula of Chmutov, Khoury and Rossi [2]. Our method is rather topological, by considering infinite cyclic cover space using a proper surface, which is not a Seifert surface. Our formula is generalized to virtual knots, giving a topological interpretation of Alexander polynomial similar to the classical case.

Although it is reasonable to assume that all diagrammatic formulas for Alexander polynomial should be transformed to each other in certain standard ways, such transformation formulas may be hard to find. We discuss this in Subsection 5.2.2. We explain the difficulty to transform between our formula and the Seifert matrix from canonical Seifert surface and that the reason for this difficulty is actually a benefit, allowing us to generalize our results to virtual knots. We manage to

find a transformation formula between our formula and the well-known formula from Wirtinger presentation. Besides, we can derive Chmutov, Khoury and Rossi's formula[2] for the second coefficient of Conway polynomial from our formula.

We remind again that Subsection 1.1 and Subsection 1.2 are logically independent. However, the parallelism between many of their results shows the idea that algebraically, a ribbon knot is like a connected sum of a virtual knot and its mirror image.

2. BACKGROUND

2.1. Alexander polynomials in $\mathbb{Z}HS^3$. Let $\mathbb{Z}HS^3$ be any integer homology sphere. Linking number is well-defined in $\mathbb{Z}HS^3$ exactly as in S^3 . Let K be a smooth knot in $\mathbb{Z}HS^3$. Then K can bound a Seifert surface F , i.e., oriented spanning surface. For a basis $[f_1], \dots, [f_{2g}]$ of $H_1(F)$, the Seifert matrix is defined as $A = (\text{lk}(f_i, f_j^\pm))_{2g \times 2g}$, where f_j^\pm denotes the push-off of cycle f_j along the \pm direction of F . Then the Conway-normalized Alexander polynomial [13] is

$$(2.1.1) \quad \Delta(t) = \left| t^{1/2}A - t^{-1/2}A^T \right|.$$

2.2. Alexander polynomial of virtual knots. Let K be a diagram for a virtual knot K , with n true crossings c_1, \dots, c_n . Orient K . For ease of presentation, we label the crossings in order of the under-crossings along K . For the over-passing arc between c_i and c_{i+1} , denote the standard meridian generator encircling it by $x_{i,i+1}$ (Here $n+1=1$). Let $x_{k(i),k(i)+1}$ be the over-passing arc at each c_i . Fig. 1 gives an $n \times n$ presentation matrix $W = \Phi - t\Psi$. For classical knots, this is the Fox free differential of Wirtinger presentation.

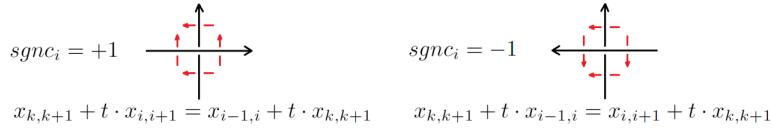


FIGURE 1. Fox differential of Wirtinger presentation.

We define the greatest common divisor of the $(n-1) \times (n-1)$ minors of W to be the Alexander polynomial for the virtual knot, denoted $\Delta_K(t)$.

Proposition 2.2.1. $\Delta_K(t)$ is a virtual knot invariant.

Proof. Track the change of W under Reidemeister moves. □

For classical knots, in fact the determinant of any $(n-1) \times (n-1)$ minor of W is the Alexander polynomial.

There are many different definitions of Alexander polynomials for virtual knots, defined from different approaches (c. f. [7]). Most of them are 2-variable. To our knowledge, the definition we give here does not appear (at least explicit) in other literature. Since we do not want to go too far on virtual knots here, the relationship between these Alexander polynomials will be discussed in detail in future work.

3. ALEXANDER MODULE OF RIBBON KNOTS IN $\mathbb{Z}HS^3$

3.1. Ribbon diagram and ribbon graph. Recall Definition 1.0.1. We shall naturally define a diagram on D^2 to represent the singularity information of the ribbon.

Definition 3.1.1. Let R be a ribbon defined in Definition 1.0.1. Label the components of singularities of the ribbon by $\alpha_1, \alpha_2, \dots, \alpha_g$. For each $i = 1, \dots, g$, let β_i be the interior component of $r^{-1}(\alpha_i)$ in D^2 and γ_i be the other component of $r^{-1}(\alpha_i)$. If one side of γ_i is at the positive normal direction of an embedded neighborhood of β_i , mark it by a small triangle, and denote the marked γ_i by $\hat{\gamma}_i$. The disk with these arcs, $(D^2, \cup_{i=1}^g \beta_i, \cup_{i=1}^g \hat{\gamma}_i)$, is the *ribbon diagram* of R .

See Fig. 2 for an example.

We introduce ribbon graph to carry informations of the ribbon diagram.

Definition 3.1.2. Let $(D^2, \cup_{i=1}^g \beta_i, \cup_{i=1}^g \hat{\gamma}_i)$ be a ribbon diagram. The pair (T, S) defined as follows is the *ribbon graph* for the ribbon diagram.

- *Ribbon tree* T : each vertex v_i is a component of $D^2 - \cup_{i=1}^g \gamma_i$ for $i = 1, \dots, g+1$, and each directed edge E_i corresponds to $\hat{\gamma}_i$ for $i = 1, \dots, g$ so that the head of E_i contains the mark triangle of $\hat{\gamma}_i$ and the tail of E_i is the other component whose boundary contains γ_i .
- *Singularity map* S : a map from the edge set of T to the vertex set of T such that $S(E_i) = v_j$ if and only if β_i is in v_j .

Note that each $\hat{\gamma}_i$ separates D^2 . We point out that there may be different ribbon diagrams corresponding to one ribbon graph. But if T is embedded in a plane, then ribbon graphs correspond bijectively to ribbon diagrams up to homeomorphism.

3.2. Half Alexander polynomial and the main theorem. We define a *ribbon matrix* $\rho_{g \times g}$ in terms of the ribbon graph. For each $i = 1, \dots, g$, subdivide E_i . Denote the new vertex by v_{E_i} and the obtained directed tree by T_{E_i} . Let P_i be the unique path in T_{E_i} from v_{E_i} to $S(E_i)$. Let

$$(3.2.1) \quad \rho_{ii} = \begin{cases} \frac{1}{2}, & \text{if the first edge of } P_i \text{ is a forward arc;} \\ -\frac{1}{2}, & \text{if the first edge of } P_i \text{ is a reverse arc.} \end{cases}$$

$$\rho_{ji} = \begin{cases} 1, & \text{if } E_j \text{ is a forward arc of } P_i; \\ -1, & \text{if } E_j \text{ is a reverse arc of } P_i; \\ 0, & \text{if } E_j \notin P_i. \end{cases} \quad \forall j \neq i.$$

Set matrix $R(t)_{g \times g} = (t-1)\rho - \frac{1}{2}(t+1)I$. That is,

$$(3.2.2) \quad R_{ii}(t) = \begin{cases} -1, & \text{if the first edge of } P_i \text{ is a forward arc;} \\ -t, & \text{if the first edge of } P_i \text{ is a reverse arc.} \end{cases}$$

$$R_{ji}(t) = \begin{cases} t-1, & \text{if } E_j \text{ is a forward arc of } P_i; \\ 1-t, & \text{if } E_j \text{ is a reverse arc of } P_i; \\ 0, & \text{if } E_j \notin P_i. \end{cases} \quad \forall j \neq i.$$

We define the *half Alexander polynomial* of the oriented ribbon R to be $A_R(t) = |R(t)|$.

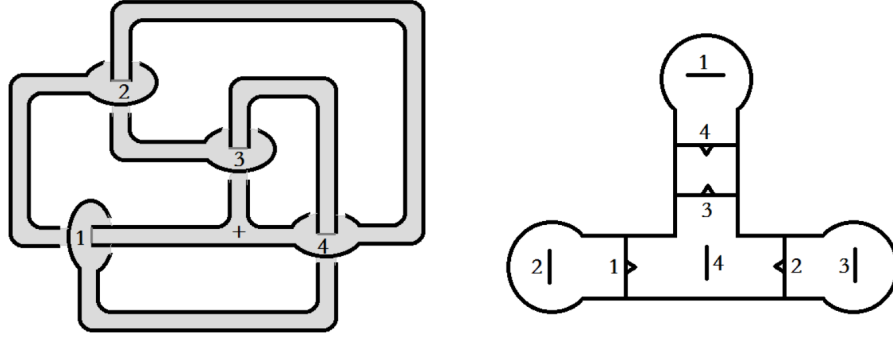


FIGURE 2. A ribbon and its ribbon diagram.

Lemma 3.2.1. *Half Alexander polynomial $A_R(t)$ is an invariant of the oriented ribbon R up to ambient isotopy of $\mathbb{Z}HS^3$.*

Proof. $R(t)_{g \times g}$ is determined by the ribbon graph, and $|R(t)|$ is independent of the labels of edges in the ribbon tree. \square

We remark that the half Alexander polynomial of the ribbon with the other orientation is $(-t)^g |R(t^{-1})|$.

Theorem 3.2.2. *Given a ribbon R for a ribbon knot K in $\mathbb{Z}HS^3$, let $A_R(t)$ be the half Alexander polynomial determined by the ribbon graph. Then the Conway-normalized Alexander polynomial of K is $\Delta(t) = A_R(t)A_R(t^{-1})$.*

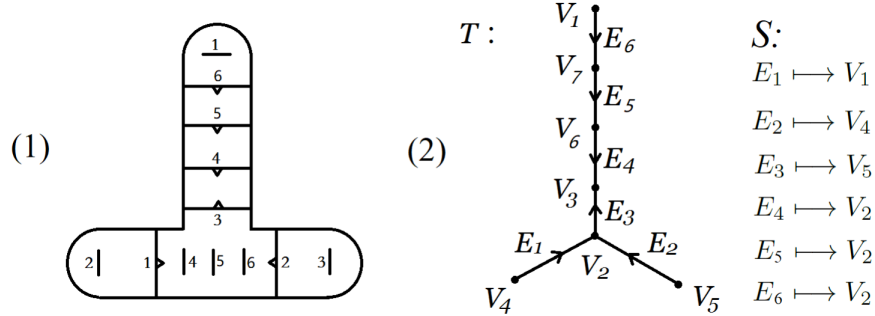


FIGURE 3. A ribbon diagram and its ribbon graph.

Example 3.2.3. For the ribbon in Fig. 3(1), the ribbon graph (T, S) is as shown in Fig. 3 and also Fig. 4. By the formula (3.2.1), the ribbon matrix should be

$$\rho = \begin{pmatrix} \frac{1}{2} & -1 & 0 & 0 & 0 & 0 \\ 0 & \frac{1}{2} & -1 & 0 & 0 & 0 \\ 1 & 0 & -\frac{1}{2} & -1 & -1 & -1 \\ -1 & 0 & 0 & \frac{1}{2} & 1 & 1 \\ -1 & 0 & 0 & 0 & \frac{1}{2} & 1 \\ -1 & 0 & 0 & 0 & 0 & \frac{1}{2} \end{pmatrix}.$$

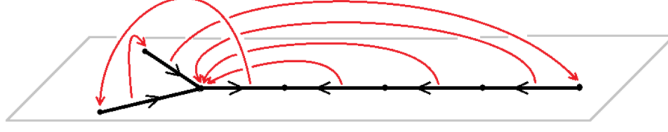


FIGURE 4. Ribbon graph drawn in a 3 dimensional manner.

Thus the half Alexander polynomial is

$$A_R(t) = |(t-1)\rho - \frac{1}{2}(t+1)I| = t(1+t^2-3t^3+3t^4-t^5),$$

and we get the Conway-normalized Alexander polynomial

$$\Delta(t) = -t^{-5} + 3t^{-4} - 4t^{-3} + 7t^{-2} - 15t^{-1} + 21 - 15t + 7t^2 - 4t^3 + 3t^4 - t^5.$$

The following corollary generalizes Lamm's Theorem 2.6 in [11] on determinants of symmetric unions.

Corollary 3.2.4. *The determinant of a ribbon knot is independent of the directions of edges in the ribbon tree for any ribbon.*

Proof. For any ribbon knot K and its ribbon R , apply formula (3.2.2) to $\det K = \Delta(-1) = |R(-1)|^2$. \square

3.3. Proof of Theorem 3.2.2.

3.3.1. *From ribbon to Seifert surface.* Let K be a ribbon knot with ribbon $r(D^2)$. We first desingularize the ribbon to get a Seifert surface for K . Let α_i be a singularity component, where $i = 1, \dots, g$.

- (1) Cut along α_i in the orientation-preserving way and deform the surface locally, which produces a hole and two ribbon-ends.
- (2) Slide the edge of a ribbon-end along the boundary of the hole towards an arc near the other ribbon-end.

The resulting surface is a Seifert surface for K of genus g , denoted F_g . See Fig. 5 for demonstration.

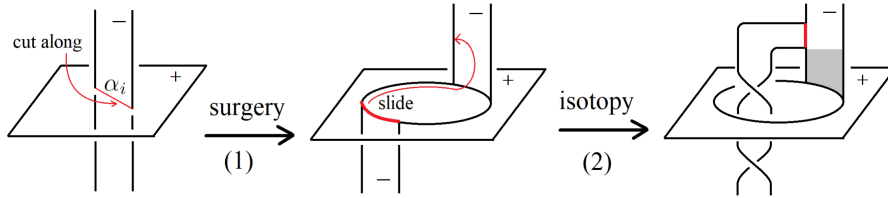


FIGURE 5. Surgery and isotopy.

It is desirable to view F_g from the ribbon diagram. On the ribbon diagram, for each $i = 1, \dots, g$,

- (1) Cut along β_i to produce a hole, say $\hat{N}(\beta_i)$.

- (2) Choose an arc in $\partial N(\beta_i)$ and an arc in ∂D^2 containing exactly one endpoint of γ_i , and glue the two arcs in the orientation-preserving way.

It is easy to see that the surface obtained is F_g , as shown in Fig. 6(2).

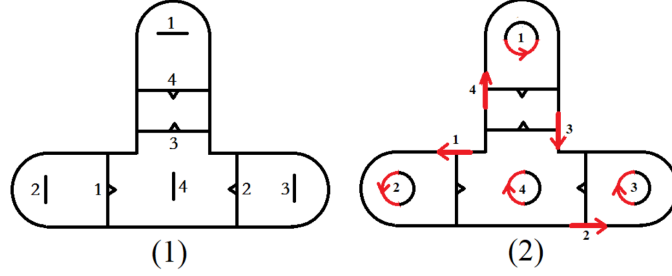


FIGURE 6. A ribbon, a representation of F_g on ribbon diagram.

3.3.2. *Homological basis on F_g .* To calculate the Seifert matrix of F_g , we first choose a standard basis of $H_1(F_g)$ based on the representation of F_g on the ribbon diagram. For each $i = 1, \dots, g$,

- (1) Let e_i be a simple closed curve encircling $\partial N(\beta_i)$, oriented counterclockwise as seen from the positive side of D^2 .
- (2) Let u_i be an interior point of γ_i , and denote the subarc of γ_i from the glued endpoint of γ_i to u_i by γ_{i0} .
- (3) On the ribbon diagram, let f_i be a path from u_i to its corresponding point in β_i . On F_g , let f_i be the path composed by γ_{i0} and f_i .

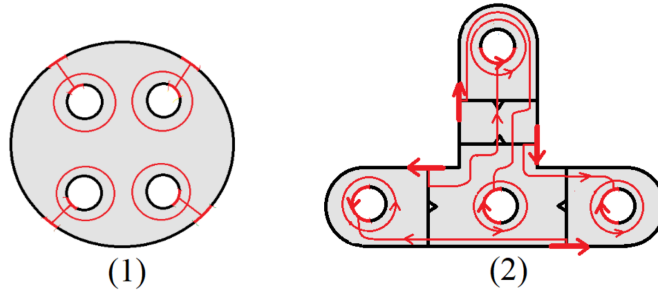


FIGURE 7. A homological basis on F_g

Choose f_i 's mutually disjoint and view them as loops in F_g , as demonstrated in Fig. 7(2). Then $[e_1], \dots, [e_g], [f_1], \dots, [f_g]$ form a standard basis of $H_1(F_g)$ with intersection form

$$(3.3.1) \quad \begin{pmatrix} O & I_{g \times g} \\ -I_{g \times g} & O \end{pmatrix}.$$

A more accurate way to view F_g and the homological basis from the ribbon is as illustrated in Fig. 8. The boundary of the gray disk contacts an endpoint of β_i .

After desingularization, the gray disk is dug and deformed to a sector. We glue it between the severed γ_i to get Fig. 7(2).

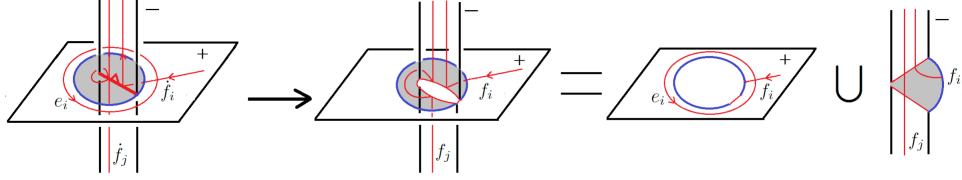


FIGURE 8. Glue along the blue arc.

3.3.3. *Seifert matrix.* Recall the definition of the Seifert matrix (c.f. [10, 11]). Choose the basis $[e_1], \dots, [e_g], [f_1], \dots, [f_g]$ of $H_1(F_g)$ as above. Notice that $\text{lk}(e_i, e_j^+) = 0$ for any $i, j = 1, \dots, g$. The Seifert matrix of F_g has the form

$$(3.3.2) \quad A = \begin{pmatrix} O & P \\ Q & L \end{pmatrix},$$

where

$$P = (\text{lk}(e_i, f_j^+))_{g \times g}, \quad Q = (\text{lk}(f_i, e_j^+))_{g \times g}, \quad L = (\text{lk}(f_i, f_j^+))_{g \times g}.$$

Our main task is to calculate P and Q .

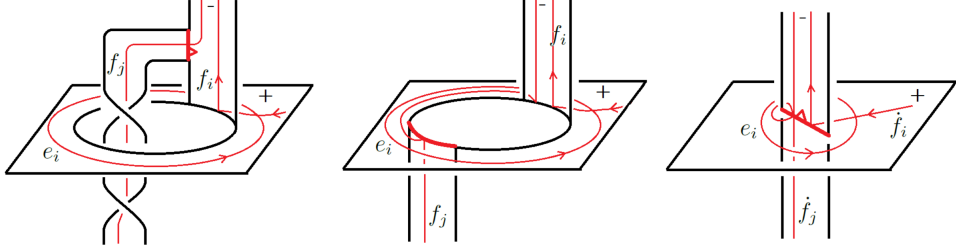


FIGURE 9. Homological basis locally represented on F_g and on the ribbon.

Near each singularity α_i , we depict f_i and an arbitrarily other f_j on F_g in Fig. 9. We have the following observations.

For any $i \neq j$,

$$(3.3.3) \quad \text{lk}(e_i, f_j^+) = \text{lk}(e_i^+, f_j) = \text{lk}(e_i, \dot{f}_j),$$

where \dot{f}_j is viewed as a loop on the ribbon. Consider a point in $\dot{f}_j \cap \gamma_i$. If \dot{f}_j passes through γ_i at this point in the same direction as the mark of γ_i , take the sign at this point as $+1$; if the direction is opposite to the mark of γ_i , take the sign as -1 . Then $\text{lk}(e_i, \dot{f}_j)$ equals the sum of signs at the intersection points of $\dot{f}_j \cap \gamma_i$. Notice that each γ_i separates D^2 . As a result, we obtain

$$(3.3.4) \quad \text{lk}(e_i, \dot{f}_j) = \begin{cases} 1, & \text{if } \beta_j \text{ belongs to the marked side of } \hat{\gamma}_i, \text{ but } \gamma_j \text{ is not;} \\ -1, & \text{if } \gamma_j \text{ belongs to the marked side of } \hat{\gamma}_i, \text{ but } \beta_j \text{ is not;} \\ 0, & \text{if } \beta_j \text{ and } \gamma_j \text{ belong to the same side of } \hat{\gamma}_i. \end{cases}$$

For $i = 1, \dots, g$, a similar argument, the details of which we omit, suggests that

$$\text{lk}(e_i, f_i^+) = 0, \quad \text{lk}(f_i, e_i^+) = 1$$

if β_i belongs to the marked side of $\hat{\gamma}_i$;

$$\text{lk}(e_i, f_i^+) = -1, \quad \text{lk}(f_i, e_i^+) = 0$$

if β_i belongs to the unmarked side of $\hat{\gamma}_i$.

3.3.4. Read from ribbon graph. Recall that given a Seifert matrix A , the Conway-normalized Alexander polynomial [13] is defined as

$$(3.3.5) \quad \Delta(t) = |t^{\frac{1}{2}}A - t^{-\frac{1}{2}}A^T|.$$

Substituting (3.3.2) into (3.3.5) gives

$$(3.3.6) \quad \Delta(t) = |t^{\frac{1}{2}}A - t^{-\frac{1}{2}}A^T| = |tP - Q^T|.$$

Reading P and Q from the ribbon graph (T, S) , we then obtain

$$(3.3.7) \quad P = \rho - \frac{1}{2}I, \quad Q = \rho^T + \frac{1}{2}I.$$

Therefore $tP - Q^T = R(t)$. This completes the proof of Theorem 3.2.2.

3.4. Alexander Invariants of ribbon knots. In this subsection, we focus on information other than the Alexander polynomial obtained from the Alexander module. By (3.3.2), we have a presentation matrix of the Alexander module for the ribbon knot

$$(3.4.1) \quad tA - A^T = \begin{pmatrix} O & tP - Q^T \\ tQ - P^T & (t-1)L \end{pmatrix} = \begin{pmatrix} O & R(t) \\ -tR(t^{-1})^T & (t-1)L \end{pmatrix}.$$

According to [1], if we sacrifice the symmetry of matrix L , L can be replaced by $\hat{L} \pm QP$, where $\hat{L} = (\text{lk}(\hat{f}_i, \hat{f}_j^+))_{g \times g}$ is symmetric. It is easy to convince that by twining and twisting the partial bands of a ribbon (changing the knot type), one can take any symmetric integer matrix to be \hat{L} . Similarly, L in (3.4.1) can be an arbitrary symmetric integer matrix. As the ribbon diagram only determines $R(t)$, ribbon knots with the same ribbon diagram may have different Alexander invariants.

3.4.1. Ribbon diagram does not determine Alexander invariants. It is known that the ribbon knots 6_1 and 9_{46} have the same Alexander polynomial but different second elementary ideals (c.f. [13]).

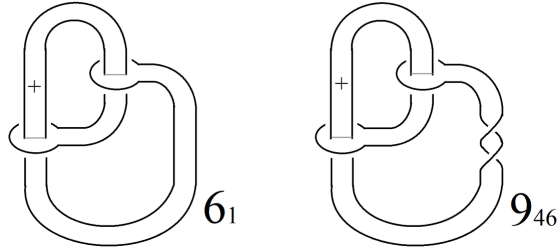


FIGURE 10. Ribbon for 6_1 and ribbon for 9_{46} .

Example 3.4.1. If we use the ribbons for 6_1 and for 9_{46} given in Fig. 10, we get two $tA - A^T$ only different in the block $(t-1)L$,

$$\begin{pmatrix} 0 & 0 & -1 & 1-t \\ 0 & 0 & 1-t & -1 \\ t & 1-t & 1-t & 0 \\ 1-t & t & 0 & 0 \end{pmatrix}_{n \times n}, \quad \begin{pmatrix} 0 & 0 & -1 & 1-t \\ 0 & 0 & 1-t & -1 \\ t & 1-t & 0 & 0 \\ 1-t & t & 0 & 0 \end{pmatrix}.$$

We can calculate that $\Delta_{6_1}(t) = \Delta_{9_{46}}(t) = 2t^{-1} - 5 + 2t$, but the second Alexander ideals of 6_1 and 9_{46} are $\langle 1 \rangle$ and $\langle t+1, 3 \rangle$ respectively.

3.4.2. Blanchfield pairing. Blanchfield pairing is a sesquilinear pairing on the Alexander module which takes values in $\mathbb{Q}(t)/\mathbb{Z}[t, t^{-1}]$. According to [5], under the dual basis of a homological basis of a Seifert surface, a presentation matrix of the Blanchfield pairing is $(t-1)(A - tA^T)^{-1}$, where A is the Seifert matrix. Therefore, for ribbon knots, using (3.3.2), after calculation, we can present the Blanchfield pairing in terms of $R(t)$ and L as

$$\mathbb{Z}[t, t^{-1}]^{2g}/(tA - A^T) \times \mathbb{Z}[t, t^{-1}]^{2g}/(tA - A^T) \longrightarrow \mathbb{Q}(t)/\mathbb{Z}[t, t^{-1}],$$

$$(v, w) \mapsto v^T (t-1) \begin{pmatrix} -R(t)^{-T} & O \\ O & I \end{pmatrix} \begin{pmatrix} (t-1)L & I \\ I & O \end{pmatrix} \begin{pmatrix} t^{-1}R(t^{-1})^{-1} & O \\ O & I \end{pmatrix} \bar{w},$$

which also depends on L .

4. HALF ALEXANDER POLYNOMIALS OF RIBBONS.

Half Alexander polynomial is a definite integer-coefficient polynomial defined for an oriented ribbon. We study half Alexander polynomials deeper in this section, emphasizing on two simplified formulas to compute half Alexander polynomials.

4.1. Example: $\Delta_{K_1}(t) = \Delta_{K_2}(t)$ but $A_{R_1}(t) \neq A_{R_2}(t)$. We show by example that half Alexander polynomial carries more information than Alexander polynomial for ribbons even up to multiplication by $\pm t^{\pm n}$ and changing t by t^{-1} .

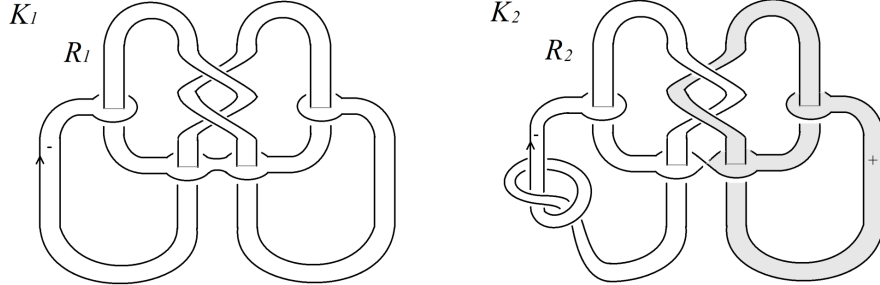


FIGURE 11. Ribbon knot K_1 with ribbon R_1 and ribbon knot K_2 with ribbon R_2 .

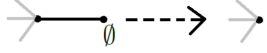


FIGURE 12. R0-reduction.

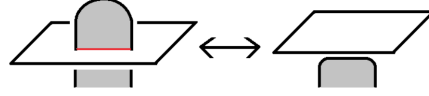


FIGURE 13. Ribbon 0-move.

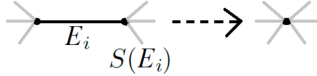


FIGURE 14. R1-reduction.

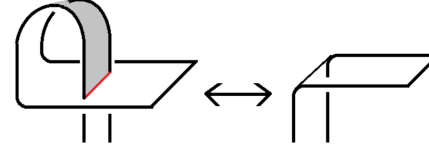


FIGURE 15. Ribbon 1-move.

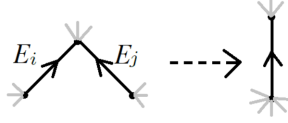


FIGURE 16. F-reduction.

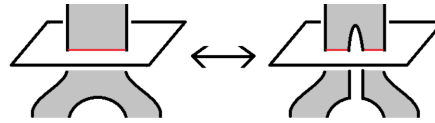


FIGURE 17. Finger move.

Example 4.1.1. There exist different ribbon knots with the same Alexander polynomial but having ribbons with different half Alexander polynomial. See Fig. 11 for two ribbon knots and their ribbons. In fact, $A_{R_1}(t) = 1 - 4t + 4t^2$ and $A_{R_2}(t) = -2t + 5t^2 - 2t^3$. But $\Delta_{K_1}(t) = \Delta_{K_2}(t) = (2t^{-1} - 5 + 2t)^2$. It can be verified that K_1 is hyperbolic, while K_2 is a satellite knot, so they are different knots.

4.2. Topological meaning of half Alexander polynomials. It is basic to ask for a topological meaning of matrix $R(t)$ and $A_R(t) = |R(t)|$. We give a 3-dimensional explanation for them.

Proposition 4.2.1. *In the Alexander module of a ribbon knot K with ribbon R , the submodule generated by e_1, \dots, e_g has presentation matrix $R(t^{-1})^T$, and thus $A_R(t^{-1})$ is a generator of the first elementary ideal, which is principal, of this submodule.*

Proof. By (3.4.1), $-tR(t^{-1})^T$ is a presentation matrix of the submodule generated by e_1, \dots, e_g . \square

Our explanation is essentially different from the folklore result that $A_R(t)$ is the Alexander polynomial of the ribbon in B^4 . In fact the latter come from the generators f_1, \dots, f_g and $R(t)$ in (3.4.1).

4.3. Reductions. We introduce four transformations for ribbon graphs. Let (T, S) be a ribbon graph defined as above.

R0-reduction: If v_i is a pendant vertex of T and $v_i \notin \text{Im}(S)$, delete v_i from T to get a new directed tree, as shown in Fig. 12. Let the new singularity map be the original S restricted to the edges of the new directed tree.

R1-reduction: If $S(E_i)$ is an end of E_i , contract E_i to get a new directed tree, as shown in Fig. 14. Let the new singularity map be S restricted to the edges of the new directed tree and if an edge was mapped to an end of E_i , we now map it to the new vertex.

F-reduction: Suppose E_i and E_j have the common head or the common tail, and $S(E_i) = S(E_j)$. Identify the other ends of E_i and E_j to get a new directed tree. If an edge was mapped to one of these two ends, we now map it to the new vertex. Fig. 16 shows the change of T when E_i and E_j have the common head.

R3-transformation: Suppose v_q is of degree 2 with $v_q \notin \text{Im}(S)$, v_q is the head of E_j , the other edge incident to v_q is E_k , and $S(E_i) = S(E_j)$ where the head of E_i is $S(E_k)$. Interchange E_j and E_k to get a new directed tree. Revise the singularity map by mapping E_k to the tail of E_i . Such transformation of (S, T) and its reverse are both called R3-transformation. See Fig. 18.

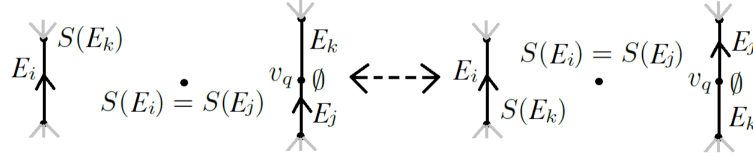


FIGURE 18. R3-reduction.

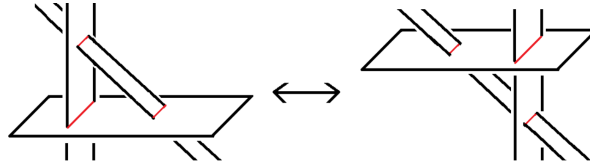


FIGURE 19. Ribbon 3-move.

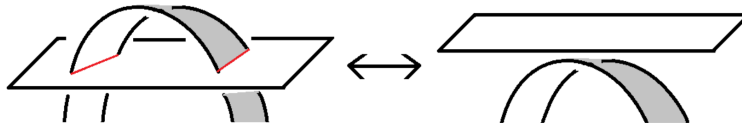


FIGURE 20. Ribbon 2-move.

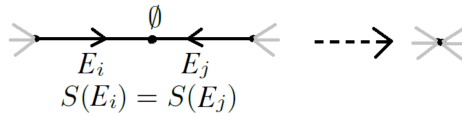


FIGURE 21. R2-reduction.

Lemma 4.3.1. *Under each of the above transformations, the half Alexander polynomial $A_R(t)$ changes by a multiplication with ± 1 or $\pm t^{\pm 1}$, and thus the Conway-normalized Alexander polynomial keeps unchanged.*

Proof. Verify by tracking the change of ribbon matrix. □

We also define several transformations of the ribbon without changing the ribbon knot type. They are *ribbon 0-move* as illustrated in Fig. 13, *ribbon 1-move* as illustrated in Fig. 15, *finger move* as illustrated in Fig. 17 and *ribbon 3-move* as illustrated in Fig. 19. It is straightforward to show that these moves induce R0-, R1-, F-reductions and R3-transformation on the ribbon graph respectively.

Remark 4.3.2. The Ribbon 2-move as shown in Fig. 20 can be easily viewed as a combination of a ribbon 0-move and a finger move. Similarly, the R2-reduction as defined in Fig. 21 is a combination of R0-reduction and F-reduction.

R0-reduction of the ribbon graph corresponds exactly to ribbon 0-move of the ribbon. However, we point out that R1-, F-reduction and R3-transformation are not necessarily obtained from ribbon 1-move, finger move, and ribbon 3-move respectively. Therefore the following corollary is not trivial.

Corollary 4.3.3. *For a ribbon knot K , the breath of $\Delta(t)$ is no bigger than twice the number of edges of T after R0-, R1-, F-reductions and R3-transformations for any ribbon for K .*

4.3.1. *General procedure from ribbon to Alexander polynomial.* We now give a general procedure computing Conway-normalized Alexander polynomial of a ribbon knot from its ribbon diagram. Let $(D^2, \cup_{i=1}^g \beta_i, \cup_{i=1}^g \tilde{\gamma}_i)$ be a ribbon diagram.

Input: Ribbon graph (T, S) .

- (1) Perform R0-, R1-, and F-reductions on (T, S) ;
- (2) Use formula (3.2.1) to get the matrix ρ ;
- (3) Compute polynomial $A_R(t) = |(t-1)\rho - \frac{1}{2}(t+1)I|$.

Output: Conway-normalized Alexander polynomial $\Delta(t) = A_R(t)A_R(t^{-1})$.

Remark 4.3.4. R3-transformation does not reduce (T, S) directly, but sometimes produces new (T, S) where R0-, R1-, or R2-reductions can be performed.

4.4. **Contracted ribbon graph and contracted formula.** The local configurations as in Fig. 22(1) frequently occur in a ribbon diagram, so it is convenient to define a contracted ribbon graph as in Fig. 22(2).

Definition 4.4.1. Let (T, S) be a ribbon graph. The pair (T^ω, S) defined as follows is the *contracted ribbon graph*.

- *Weighted tree T^ω :* For each maximal induced directed path P in T whose edges are mapped by S to the same vertex and whose interior vertices are not in $\text{Im}(S)$, replace P in T by an edge E with the same direction and endpoints as P , and label E with the length of P as its **weight**, denoted $\omega(E)$.
- *Singularity map S :* Map each edge of T^ω to the image of its original path under T .

Using R2-reduction in Fig. 21, to compute Alexander polynomial, we can actually further contract the ribbon graph by replacing "maximal induced directed

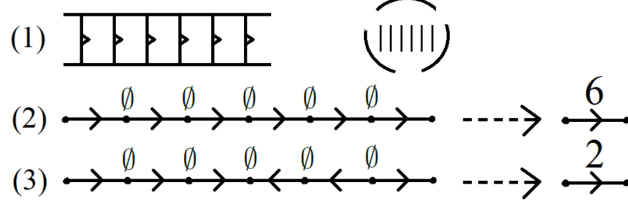


FIGURE 22. Contracted ribbon graph.

path” in the definition of weighted tree by ”maximal induced path”, as shown in Fig. 22(3).

Using contracted ribbon graph, we give a variant formula to compute half Alexander polynomial of ribbons, usually simpler in practice.

We define a matrix $\mathbf{R}(t)$ from a contracted ribbon graph. For each edge E_i in T^ω , subdivide it. Denote the new vertex by v_{E_i} and the obtained directed tree by T_{E_i} . Let P_i be the unique path in T_{E_i} from v_{E_i} to $S(E_i)$. Let

$$(4.4.1) \quad \mathbf{R}_{ii}(t) = \begin{cases} -1, & \text{if the first edge of } P_i \text{ is a forward arc;} \\ -t, & \text{if the first edge of } P_i \text{ is a reverse arc.} \end{cases}$$

$$\mathbf{R}_{ji}(t) = \begin{cases} t^{\omega_i} - 1, & \text{if } E_j \text{ is a forward arc of } P_i; \\ 1 - t^{\omega_i}, & \text{if } E_j \text{ is a reverse arc of } P_i; \quad \forall j \neq i, \\ 0, & \text{if } E_j \notin P_i. \end{cases}$$

where ω_i is the weight of E_i .

Theorem 4.4.2. *The half Alexander polynomial $A_R(t) = \pm |(\mathbf{R}_{ji}(t))|$.*

Proof. We begin by considering ribbon graph (T, S) . After relabelling, for simplification of notations, we may assume $\hat{\gamma}_1, \hat{\gamma}_2, \dots, \hat{\gamma}_\omega$ are successive arcs in the ribbon diagram as in Fig. 22(1) so that the path $E_1 E_2 \dots E_\omega$ in T corresponds to an edge E in T^ω with $\omega = \omega(E)$. We may assume $\hat{\gamma}_2, \dots, \hat{\gamma}_\omega$ are in the path P_1 defined in Subsection 3.2.

Suppose $\hat{\gamma}_1$ is a forward arc of P_1 . By (3.2.2), the minor

$$(4.4.2) \quad (\mathbf{R}_{ji}(t))_{1, \dots, \omega; 1, \dots, \omega} = \begin{pmatrix} -1 & & & & \\ t-1 & -1 & & & \\ t-1 & t-1 & -1 & & \\ \vdots & \vdots & \vdots & \ddots & \\ t-1 & t-1 & t-1 & \cdots & -1 \end{pmatrix}.$$

It is easy to see from ribbon graph that

$$(4.4.3) \quad \begin{aligned} R_{ji}(t) &= R_{j,\omega}(t), \quad \forall j \neq 1, 2, \dots, \omega, \forall i = 1, 2, \dots, \omega; \\ R_{ji}(t) &= R_{j,\omega+1}(t), \quad \forall j = 1, 2, \dots, \omega, \forall i \neq 1, 2, \dots, \omega. \end{aligned}$$

Example 4.4.3. From the ribbon graph in Fig. 3(2), we can contract E_4, E_5 and E_6 to get a contracted ribbon graph. Then by formula (5.3.1), the matrix $(\mathbf{R}_{ji}(t))$ is

$$\mathbf{R}(t) = \begin{pmatrix} 1 & 1-t & 0 & 0 \\ 0 & 1 & 1-t & 0 \\ t-1 & 0 & -t & 1-t^3 \\ 1-t & 0 & 0 & -1 \end{pmatrix}.$$

Thus the half Alexander polynomial is

$$A_R(t) = |(\mathbf{R}_{ji}(t))| = t(1 + t^2 - 3t^3 + 3t^4 - t^5).$$

4.5. Path-type simplified formula. We give a much simpler formula for half Alexander polynomial when the ribbon tree is a path. In fact, we can use finger moves to deform any ribbon to a new ribbon so that the ribbon tree is a path.

4.5.1. Generality.

Proposition 4.5.1. *Any ribbon knot has a ribbon such that T is a path in the ribbon graph (T, S) .*

Proof. Let R be a ribbon in S^3 , and $(D^2, \cup_{i=1}^g \beta_i, \cup_{i=1}^g \hat{\gamma}_i)$ be its ribbon diagram. Note that a tree is a path if and only if it has only two pendant vertices. We use finger moves on R to decrease pendant vertices.

Let v_i be a pendant vertex of T . Let $P = E_1 E_2 \dots E_k$ be the maximal induced path in T with one endpoint v_i incident to E_1 . Then the other endpoint denoted v_j , has degree at least 3 in T . Recall that each vertex of P is a component of $D^2 - \cup_{i=1}^g \gamma_i$. The boundary of the component corresponding to v_j has an arc $a \subset r(\partial D^2)$ not intersecting $\hat{\gamma}_k$, where $\hat{\gamma}_k$ corresponds the edge E_k . Push a across $\alpha_k, \dots, \alpha_1$ in succession by finger moves in S^3 to split each of $\hat{\gamma}_k, \dots, \hat{\gamma}_1$ into two arcs, as shown in Fig. 23(1). The effect on T is to split the edges E_k, \dots, E_1 in succession until v_i has degree 2, as shown in Fig. 23(2).

Do this inductively to pendant vertices until T becomes a path. \square

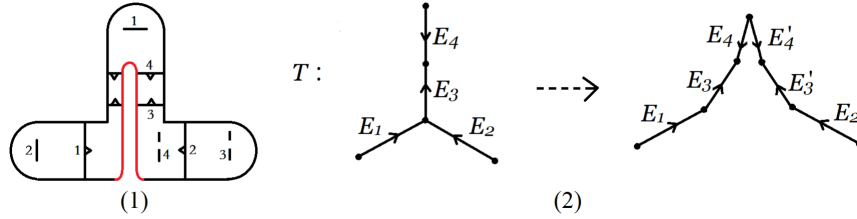


FIGURE 23. Change ribbon graph into a path.

4.5.2. Simplified formula. Let R be a ribbon with ribbon graph (T, S) where T is a path. Assume $T = v_1 v_2 \dots v_{n+1}$, and the directed edge E_i is either $v_i v_{i+1}$ or $v_{i+1} v_i$ for $i = 1, \dots, n$. Read off a matrix $W_{(n+1) \times n}(t) = W'(t) + W''(t)$ from (T, S) as follows.

$$\begin{cases} W'_{i,i}(t) = 1, W'_{i+1,i}(t) = -t, & \text{if } E_i = v_i v_{i+1}, \\ W'_{i,i}(t) = -t, W'_{i+1,i}(t) = 1, & \text{if } E_i = v_{i+1} v_i, \\ W''_{k,i}(t) = t - 1, & \text{if } S(E_i) = v_k. \end{cases}$$

and other entries are 0.

Theorem 4.5.2. $A_R(t) = \pm |W^*(t)|$, where $W^*(t)$ is $W(t)$ deleting the $(n+1)$ th row.

Proof. Let $X = \text{diag}\{\text{sgn}E_1, \dots, \text{sgn}E_n\}$, where $\text{sgn}E_i = +1/-1$ if and only if $E_i = v_i v_{i+1}/v_{i+1} v_i$. Then we have $R(t) = -X\Lambda_n W^*(t)$. One can verify this case by case depending on $\text{sgn}E_i$ and whether E_i is forward in P_i . Therefore $A_R(t) = (-1)^{|E_{i-1}|} |W^*(t)|$, where $|E_{i-1}|$ is the number of edges with $\text{sgn} = +1$ in T . \square

Remark 4.5.3. Theorem 4.5.2 has a more topological proof and $R(t) = -X\Lambda_n W^*(t)$ can be understood more topologically. We hint that one can refer to the proof of Proposition 5.2.4 to find dual homological generators, but we will not explain the details here.

4.5.3. *Geography of half Alexander polynomials.* Given an integer-coefficient polynomial $f(t)$ with $f(1) = \pm 1$, Terasaka constructed in [15] a ribbon knot whose Alexander polynomial is $f(t)f(t^{-1})$. His arguments were complicated calculations using Wirtinger representation of knot diagram. But one can verify that in fact his construction satisfies $A_R(t) = f(t)$. We give a much more compact construction of ribbons such that $A_R(t) = f(t)$ using Theorem 4.5.2. But our calculation is still inspired by Terasaka's.

Corollary 4.5.4. *For any $f(t) \in \mathbb{Z}[t]$ with $f(1) = \pm 1$, there is a ribbon diagram so that the half Alexander polynomial $A_R(t) = t^{|E_{-1}|} f(t)$, where $|E_{-1}|$ is the number of edges with $\text{sgn} = -1$ in the ribbon tree.*

Proof. First assume $f(1) = 1$. Then $F(x) = (f(t) - 1)/(t - 1)$ is a polynomial. We may suppose $F(x) = \sum_{i=0}^n a_i t^i - \sum_{j=0}^m b_j t^j$, where $a_i, b_j \geq 0$. We construct a ribbon graph (T, S) where T is a path as follows.

Let the two pendant vertices of T be *red vertex* and *blue vertex*. In Fig. 24, S maps each red/blue edge to the red/blue vertex. Start from red vertex. The first two edges are the blue edges as depicted in Fig. 24(1). Then identify the terminal vertices of the paths for a_0, \dots, a_n as shown in Fig. 24(2) in succession. If $n > m/n < m$, identify the terminal vertex of the path as shown in the upper/lower left of Fig. 24(3) and then identify the terminal vertices of the paths for b_m, \dots, b_0 as shown in the upper/lower right of Fig. 24(3) in order. Ending at the blue vertex gives the path T .

To calculate $A_R(t)$, observe the following two $(2k+1) \times (2k+1)$ blocks.

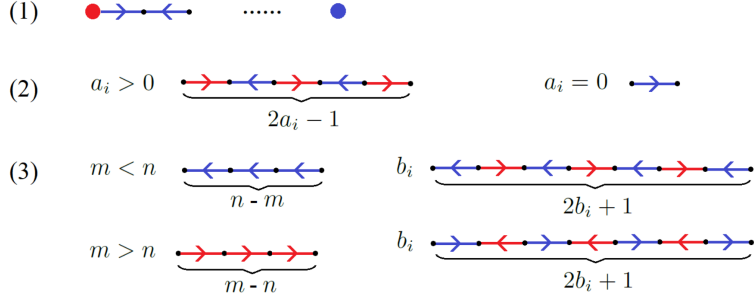


FIGURE 24. Ribbon graph.

$$\begin{pmatrix} t-1 & 0 & t-1 & \cdots & 0 & t-1 \\ \frac{1}{-t} & -t & & & & \\ & 1 & 1 & & & \\ & & -t & \ddots & & \\ & & & \ddots & -t & \\ & & & & 1 & 1 \end{pmatrix}, \begin{pmatrix} 0 & t-1 & 0 & \cdots & t-1 & 0 \\ -t & & & & & \\ 1 & 1 & & & & \\ & -t & -t & & & \\ & & & 1 & \ddots & \\ & & & & \ddots & -t \\ & & & & & 1 & 1 \end{pmatrix}$$

Multiplying the columns by $1, -1, 1, \dots, -1, 1$ in succession and adding together to the first column, the first column of the two blocks become $((k+1)(t-1), 1, 0, \dots, 0)^T$ and $(-k(t-1), 1, 0, \dots, 0)^T$ respectively. The $W_{n+1}^*(t)$ defined in Algorithm 5 is like

$$\begin{pmatrix} 1 & 0 & t-1 & 0 & t-1 & t-1 & \cdots & 0 & t-1 & 0 \\ -t & -t & & & & & & & & \\ & 1 & 1 & & & & & & & \\ & & -t & -t & & & & & & \\ & & & 1 & 1 & & & & & \\ & & & & -t & 1 & & & & \\ & & & & & -t & \ddots & & & \\ & & & & & & \ddots & -t & & \\ & & & & & & & 1 & 1 & -t \end{pmatrix}$$

Multiply the columns by $1, -1, 1, -1, 1, t, -t, \dots, t^n, t^{n-1}, \dots, t^m, -t^m, t^m, \dots, 1, -1, 1$ in succession and add together to the first column, then the first column becomes

$$\left(1 + (t-1) \left(\sum_{i=0}^n a_i t^i - \sum_{j=0}^m b_j t^j \right), 0, \dots, 0 \right)^T.$$

Thus $|W_{n+1}^*(t)| = (-t)^{|E_{-1}|} f(t)$, where $|E_{-1}|$ is the number of edges with $sgn = -1$. Eventually $A_R(t) = |-X\Lambda_n W_{n+1}^*(t)| = t^{|E_{-1}|} f(t)$.

If $f(1) = -1$, apply an inverse of R0-reduction to the ribbon diagram constructed above. \square

5. ALEXANDER POLYNOMIAL OF GENERAL KNOTS AND VIRTUAL KNOTS

5.1. **Motivation: Similarity between ribbon graph and Gauss diagram.**

Let K be an oriented knot in S^3 with a diagram \mathbb{K} . Let $-\bar{K}$ denote the reflection of K with the reversed orientation. Then the connected sum $K\#-\bar{K}$ is a ribbon knot, and we get a canonical ribbon from the diagram $\mathbb{K}\#-\bar{\mathbb{K}}$.

As illustrated in Fig. 27 and 28, from the Gauss diagram of \mathbb{K} we can always get exactly a ribbon graph as follows.

- (1) Replace the positive/negative sign at the start of each arrow by a direction on the circle consistent/inconsistent with the orientation of K ;
- (2) Merge the contiguous tips of arrows into a vertex;
- (3) Erase a small arc where the connected sum is made.

We know that

$$\Delta_{K\#-\bar{K}}(t) = \Delta_K(t)\Delta_{-\bar{K}}(t) = \Delta_K(t)\Delta_K(t) = \Delta_K(t)\Delta_K(t^{-1}).$$

On the other hand, $\Delta_{K\#-\bar{K}}(t) = A_R(t)A_R(t^{-1})$, where $R(t)$ is the half Alexander polynomial of the ribbon graph. One may wonder whether $A_R(t) = \pm t^{\pm k} \Delta_K(t)$? We prove this is true. This leads us to discover a new method for computing Alexander polynomial of general knots.

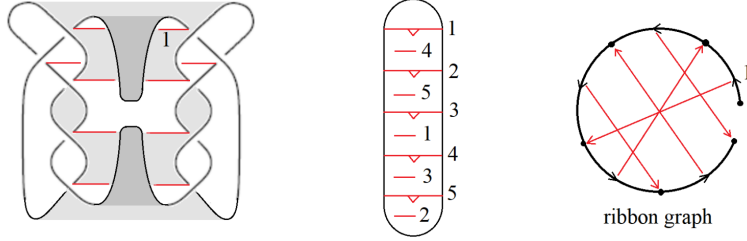


FIGURE 27. Gauss diagram and ribbon graph.

5.2. New Formulas for classical knots. Let \mathbb{K} be a diagram for a knot K in S^3 , with n crossings c_1, \dots, c_n . Let \mathbb{G} be the Gauss diagram of \mathbb{K} . Denote the circle of \mathbb{G} by C . Each crossing c_i corresponds to an arrow, still denoted c_i . Choose a base point p on C avoiding the starts and tips of all the arrows. We adopt the convention that the start of the arrow corresponds to the lower strand and the tip of the arrow corresponds to the upper strand. See Fig. 28 for an example. We give a formula for computing Alexander polynomial of K from Gauss diagram \mathbb{G} .

- (1) Denote the start of c_i by c_{i0} . For each arrow c_i , let P_i be the unique arc in $C - \{p\}$ from the start of c_i to the tip of c_i , and define the sign of P_i , denoted $sgn P_i$, to be $+1$ if P_i is counterclockwise and -1 otherwise.
- (2) Read off a matrix $\rho_{n \times n}$ as follows.

$$\rho_{ii} = \frac{1}{2} \cdot sgn c_i \cdot sgn P_i;$$

$$\rho_{ji} = \begin{cases} sgn c_j \cdot sgn P_i, & \text{if } c_{j0} \in P_i; \\ 0, & \text{if } c_{j0} \notin P_i. \end{cases} \quad \forall j \neq i.$$

Theorem 5.2.1. *The Alexander polynomial of K is the determinant of $R(t) := (t - 1)\rho - \frac{1}{2}(t + 1)I$, up to multiplication by $\pm t^{\pm k}$.*

Remark 5.2.2. According to the relationship between Gauss diagram and ribbon graph in 5.1, R0-reduction applies to simplify matrix $R(t)$. So to simplify the calculation, we can choose base point p to be adjacent to a string of consecutive undercrossings.

Example 5.2.3. For the knot 5_2 in Fig. 28, we have

$$\rho = \begin{pmatrix} 1/2 & 0 & 0 & 0 & 0 \\ 1 & 1/2 & 0 & -1 & 0 \\ 1 & 1 & 1/2 & -1 & -1 \\ 0 & 1 & 1 & -1/2 & -1 \\ 0 & 1 & 0 & 0 & -1/2 \end{pmatrix},$$

thus $\Delta(t) \doteq |R(t)| \doteq |(t - 1)\rho - \frac{1}{2}(t + 1)I| = 2t^{-1} - 3 + 2t$.

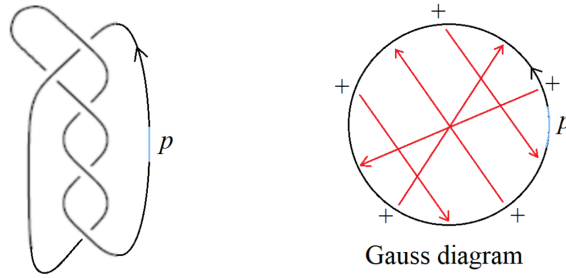


FIGURE 28. Gauss diagram.

5.2.1. *Independent Proof of Theorem 5.2.1.*

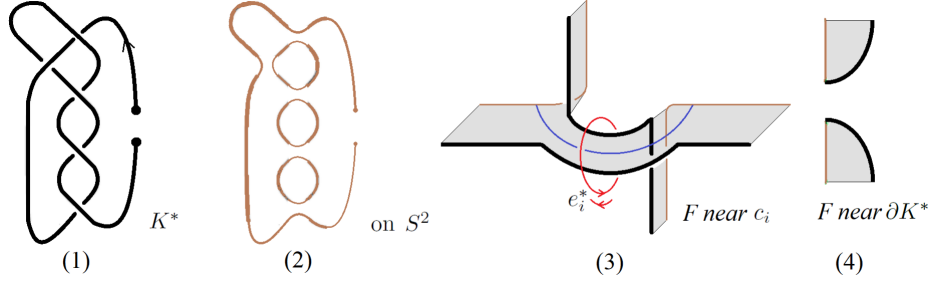
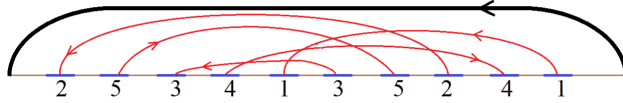
Proof. Choose a ball B^3 in S^3 so that $K - intB^3$ is an unknotted arc in $S^3 - intB^3$. Set $K^* = K \cap B^3$. Then $B^3 - N(K^*) \cong S^3 - N(K)$.

Assume K^* is contained in a collar N_B of B^3 and \mathbb{K}^* is a regular projection of K^* on $S^2 = \partial B^3$. Orient K^* . Smooth the crossings of \mathbb{K}^* in the orientation-preserving way to get Seifert circles and a Seifert arc on S^2 , as shown in Fig. 29(2).

Now we construct a surface F in N_B having the shape as drawn in Fig. 29(3) near each crossing c_i and Fig. 29(4) near the two points ∂K^* , whose boundary is the union of K^* , the Seifert circles and Seifert arc.

Let X_∞ be the infinite cyclic cover of $B^3 - N(K^*) \cong S^3 - N(K)$. Let Y be the space $(B^3 - N(K^*))$ -cut-along- F , that is, $B^3 - N(K^*) - F$ with two copies F_+ and F_- replacing the removed F . We claim that Y is a fundamental domain for the covering space X_∞ .

In fact, the boundary of $B^3 - N(K^*)$ is a torus and the Seifert circles on S^2 are trivial circles on this torus. Cap these circles by the disks they bound on S^2 one by one from innermost ones and perturb it into the interior of $B^3 - N(K^*)$, then we get a Seifert surface \bar{F} for K . It is well-known that $(B^3 - N(K^*))$ -cut-along- \bar{F} is a fundamental domain of X_∞ . We identify the difference between it and

FIGURE 29. The construction of surface F .FIGURE 30. $(B^3 - N(K^*))$ -cut-along- F vs cut-along \bar{F} .FIGURE 31. The basis f_1, \dots, f_n drawn on F cut along the blue arcs.

$(B^3 - N(K^*))$ -cut-along- F . The latter subtracting the former is the union of solid neighbourhoods of the Seifert disks on the boundary torus, as 1-handles connecting the boundary torus to \bar{F} , while the former subtracting the latter is the same solids, but as 2-handles. Thus in X_∞ , for any $i \in \mathbb{Z}$, cut off these 2-handles in the i th copy of $(B^3 - N(K^*))$ -cut-along- \bar{F} and glue them to the corresponding adjacent copy as 1-handles, then we get copies of $(B^3 - N(K^*))$ -cut-along- F . See Fig. 30.

For each crossing c_i , let e_i be a simple closed curve in $B^3 - F$ encircling the band as shown in Fig. 29(3), oriented to encircle the upper strand of K^* with a right-hand screw. Then e_1, \dots, e_n form a basis of $H_1(B^3 - F)$.

On the other hand, if cut along all the blue arcs depicted in Fig. 29(3) for the crossings, then F becomes a disk. So we may choose simple closed curves f_1, \dots, f_n on F dual to the blue arcs to form a basis of $H_1(F)$. Specifically, f_i starts from the lower strand at c_i , ends at the upper strand at c_i , and intersects the blue arc at c_i in a single point. See Fig. 31. Define the sign of f_i , denoted $sgn f_i$, to be $+1$ if the orientation of f_i is similar to that of K^* and -1 otherwise.

Notice that F is orientable, with the orientation compatible with that of K^* . Let f_i^+/f_i^- be the push-off of f_i in the positive/negative normal direction of F into $B^3 - F$. Then by tracing along f_i in Fig. 29(3), we see that, in $H_1(B^3 - F)$,

$$[f_i^+] = \sum_{j=1}^n P_{ji}[e_j], \quad [f_i^-] = \sum_{j=1}^n Q_{ij}[e_j],$$

where

$$P_{ii} = \begin{cases} 0, & \text{if } \text{sgn}f_i = \text{sgn}c_i; \\ -1, & \text{if } \text{sgn}f_i = -\text{sgn}c_i. \end{cases}$$

$$Q_{ii} = \begin{cases} +1, & \text{if } \text{sgn}f_i = \text{sgn}c_i; \\ 0, & \text{if } \text{sgn}f_i = -\text{sgn}c_i. \end{cases}$$

$$\forall j \neq i, \quad P_{ji} = Q_{ij} = \begin{cases} \text{sgn}c_j \cdot \text{sgn}f_i, & \text{if } f_i \text{ goes through the lower strand at } c_j; \\ 0, & \text{otherwise.} \end{cases}$$

The deck transformation on X_∞ corresponding to the meridian of K induces an automorphism t on $H_1(X_\infty)$. By (5.2.1), it is standard to prove that $R(t) = tP - Q^T$ is a presentation matrix for $\mathbb{Z}[t, t^{-1}]$ -module $H_1(X_\infty)$, that is, the *Alexander module*, where $P = (P_{ji})_{n \times n}$ and $Q = (Q_{ji})_{n \times n}$. Using notation in terms of Gauss diagram, we have

$$R_{ii}(t) = \begin{cases} -1, & \text{if } \text{sgn}P_i = \text{sgn}c_i; \\ -t, & \text{if } \text{sgn}P_i = -\text{sgn}c_i. \end{cases}$$

$$R_{ji}(t) = \begin{cases} t-1, & \text{if } c_{j0} \in P_i \text{ and } \text{sgn}P_i = \text{sgn}c_j; \\ 1-t, & \text{if } c_{j0} \in P_i \text{ and } \text{sgn}P_i = -\text{sgn}c_j; \\ 0, & \text{if } c_{j0} \notin P_i. \end{cases} \quad \forall j \neq i.$$

That is $R(t) = (t-1)\rho - \frac{1}{2}(t+1)I$. \square

5.2.2. Relationship with one known formula. Although we have proved Theorem 5.2.1 independently, it is still thought-provoking to make clear the relation between our formula and as many known formulas as possible.

Although F constructed in the above proof is similar to the canonical Seifert surface, it is difficult to find a general conversion relationship between our method and the Seifert surface method. The two matrices may be quite different, and the size of Seifert matrix for the canonical Seifert surface is less than n . Furthermore, our construction of F is valid for virtual knots in general, while a major difficulty in defining Alexander polynomials for virtual knots is that they cannot bound Seifert surfaces.

Nevertheless, we can make clear the relation between the two presentation matrices $R(t) = tP - Q^T$ and $W = \Phi - t\Psi$ for the Alexander module.

There is no direct linear translation between $R(t)$ and W . We need to enlarge W depending on the choice of the base point p . Assume the base point p is in the over-passing arc between c_n and c_1 , and denote the generators for the initial and last over-passing arc of $\mathbb{K} - p$ by $x_{0,1}$ and $x_{n,n+1}$ respectively, which are in fact equal.

Recall that Fig. 1 gives $W = \Phi - t\Psi$. Now let $\tilde{W} = \dot{\Phi} - t\tilde{\Psi}$ be the matrix representing relations in Fig. 1 for the long knot $\mathbb{K} - p$, that is,

$$\dot{\Phi}_{i+\frac{1}{2}(1-\text{sgn}c_i),i} = -1, \quad \dot{\Phi}_{k(i)+1,i} = 1;$$

$$\dot{\Psi}_{i+\frac{1}{2}(1+\text{sgn}c_i),i} = -1, \quad \dot{\Psi}_{k(i)+1,i} = 1,$$

and other entries are 0. Then $\tilde{W} = \dot{\Phi} - t\tilde{\Psi}$ is an enlarged and equivalent presentation matrix of $W = \Phi - t\Psi$, where $\check{\Psi} = \begin{pmatrix} \eta & \dot{\Phi}_{(n+1) \times n} \end{pmatrix}$, $\check{\Psi} = \begin{pmatrix} O_{(n+1) \times 1} & \dot{\Psi}_{(n+1) \times n} \end{pmatrix}$ and $\eta = (-1, 0 \cdots 0, 1)^T$.

Set

$$\Lambda_n = \begin{pmatrix} 1 & & & \\ 1 & 1 & & \\ \vdots & \vdots & \ddots & \\ 1 & 1 & \cdots & 1 \end{pmatrix}_{n \times n}, \quad X = \begin{pmatrix} sgnc_1 & & & \\ & sgnc_2 & & \\ & & \ddots & \\ & & & sgnc_n \end{pmatrix}.$$

Proposition 5.2.4. $R(t) = -X\Lambda_n\tilde{W}^*$, where $\tilde{W}^* = \dot{\Phi}^* - t\tilde{\Psi}^*$ is $\tilde{W} = \dot{\Phi} - t\tilde{\Psi}$ deleting the $(n+1)$ th row.

Remark 5.2.5. It is always incorrect that $R(t) = -X\Lambda_n W$, as $|W| = 0$.

Proof. This can be directly verified. But we prefer to give a more comprehensible proof here.

Choose generators $x_{i-1,i} - x_{n,n+1}$, $i = 1, \dots, n$ for Alexander module, then \tilde{W} deleting the last row is a presentation matrix for Alexander module. We further have the following subtle observation.

Claim: \tilde{W}_{n+1}^* is a presentation matrix for Alexander module.

In fact, the first relation $x_{0,1} - x_{n,n+1} = 0$ is a linear combination of the relations from the second to the $n+1$ th columns multiplying some suitable t^{k_i} 's. The proof is similar to that in $W = \Phi - t\Psi$, one column is a linear combination of the other columns multiplied with suitable t^{k_i} 's.

Introduce equivalent generators $\delta_i = x_{i,i+1} - x_{i-1,i}$ for $i = 1, \dots, n$. Then

$$(x_{0,1} - x_{n,n+1}, \dots, x_{n-1,n} - x_{n,n+1}) = -(\delta_1, \dots, \delta_n)\Lambda_n.$$

Set elements $e_i = x_{k(i),k(i)+1} - x_{i-sgnc_i,i}$ for $i = 1, \dots, n$. Then the relations of the columns of \tilde{W} are equivalent to

$$(t-1)e_i - sgnc_i \cdot t \cdot \delta_i = 0.$$

This implies that in the Alexander module, which is a torsion module, $(t-1)e_i$, $i = 1, \dots, n$ are equivalent to δ_i , $i = 1, \dots, n$, which further implies that e_1, \dots, e_n form generators for the Alexander module.

We aim to show for the Alexander module, under generators e_1, \dots, e_n , our $R(t)$ is a presentation matrix. The relations of \tilde{W} are also equivalent to $e_i - t(x_{k(i),k(i)+1} - x_{i+sgnc_i,i}) = 0$, that is,

$$(e_1, \dots, e_n) = t(x_{0,1} - x_{n,n+1}, \dots, x_{n-1,n} - x_{n,n+1})\dot{\Psi}^*.$$

Combining (5.2.2) and (5.2.3), we get

$$(e_1, \dots, e_n) = -(\delta_1, \dots, \delta_n)\Lambda_n\dot{\Psi}^* = -(e_1, \dots, e_n)(t-1)X\Lambda_n\dot{\Psi}^*.$$

We obtain a presentation matrix $I_n + (t-1)X\Lambda_n\dot{\Psi}^*$. Noticing that $\dot{\Psi}^* - \dot{\Phi}^* = \Lambda_n^{-1}X$, this matrix equals $-R(t)$. \square

5.2.3. Relationship with Polyak-Viro Formula. As an application of our formula, we can derive Chmutov, Khoury and Rossi's formula[2] at least for the second coefficient \mathbf{c}_2 of Conway polynomial.

Corollary 5.2.6. Let \mathbb{G} be a Gauss diagram for a knot K . Then \mathbf{c}_2 is the signed sum of the sub-Gauss diagrams of \mathbb{G} as shown in Fig. 32.

Remark 5.2.7. The directions of the arrows in our formula is the opposite of those in the formula in [2], with the same signs. It is clear, however, that the resulting \mathbf{c}_2 takes the same value.

Proof. Let $\Delta(t)$ be the Conway-normalized Alexander polynomial for a knot, then we know that $\Delta(1) = 1$, $\Delta'(1) = 0$ and $\Delta''(1) = 2\mathbf{c}_2$.

Recall that $|R(t)| \doteq \Delta(t)$. As $|R(1)| = (-1)^n$, we have $|R(t)| = (-1)^n t^k \Delta(t)$ for some $k \in \mathbb{N}$. We first determine k .

Claim: k is the number of diagonal elements $-t$.

In fact, $|R(t)'|_{t=1} = (-1)^n [k t^{k-1} \Delta(t) + t^k \Delta'(t)]|_{t=1} = (-1)^n k$. On the other hand, taking the derivative of $R(t)$ column by column and letting $t = 1$, by (3.0.1), we obtain $|R(t)'|_{t=1}$ is $(-1)^n$ multiplying the number of diagonal elements $-t$.

Now we divide each column of $R(t)$ by the corresponding diagonal element -1 or $-t$ and we obtain a matrix $\mathcal{R}(t)$ as follows, which now satisfies $|\mathcal{R}(t)| = \Delta(t)$.

$$(5.2.1) \quad \mathcal{R}_{ii}(t) = 1.$$

$$(5.2.2) \quad \mathcal{R}_{ji}(t) = \begin{cases} 1 - e^{\text{sgn} P_i \text{sync}_i}, & \text{if } c_{j0} \in P_i \text{ and } \text{sync}_i = \text{sync}_j; \\ t^{\text{sgn} P_i \text{sync}_i} - 1, & \text{if } c_{j0} \in P_i \text{ and } \text{sync}_i = -\text{sync}_j; \quad \forall j \neq i. \end{cases}$$

$$(5.2.3) \quad 0, \quad \text{if } c_{j0} \notin P_i.$$

Recall that $\mathbf{c}_2 = \frac{1}{2} |\mathcal{R}(t)''|_{t=1}$. Let X^{ij} be the matrix obtained by taking the derivatives of the i th and j th columns of $\mathcal{R}(t)$ and letting $t = 1$. A simple calculation gives $\frac{1}{2} |\mathcal{R}(t)''|_{t=1} = \sum_{i < j} |X^{ij}|$. As $\mathcal{R}(1) = I_n$, it is easy to see that $|X^{ij}| = |X_{i,j;i,j}^{ij}|$, where $X_{i,j;i,j}^{ij}$ is the 2×2 submatrix of X^{ij} formed by the i th and j th rows and columns.

It remains to compute each $|X_{i,j;i,j}^{ij}|$. From (5.2.1) we can calculate

$$(5.2.4) \quad \mathcal{R}'_{ii}(1) = 0.$$

$$(5.2.5) \quad \mathcal{R}'_{ji}(1) = \begin{cases} -\text{sgn} P_i \text{sync}_j, & \text{if } c_{j0} \in P_i; \\ 0, & \text{if } c_{j0} \notin P_i. \end{cases} \quad \forall j \neq i.$$

Using this formula, it is easy to complete the proof by discussing the value of $|X_{i,j;i,j}^{ij}|$ according to the directions and signs of the i th and j th arrows. \square

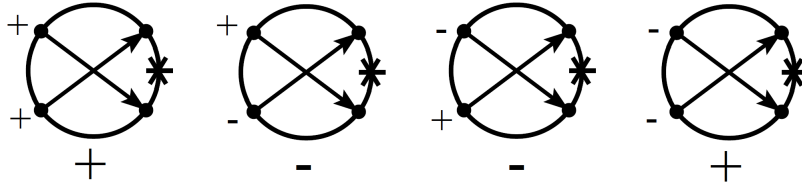


FIGURE 32. Arrow diagrams and their signs to compute \mathbf{c}_2 .

5.3. New formula and contracted formula for virtual knots.

5.3.1. *New formula.* Let \mathbb{K} be a diagram for a virtual knot K , with n true crossings c_1, \dots, c_n . Let \mathbb{G} be the Gauss diagram of \mathbb{K} . Note that the claim in the proof of Proposition 5.2.4 does not hold in general for virtual knots. Choose p_i be a base point in the interior of the over-passing arc between c_i and c_{i+1} , very close to c_i . Then we have a determinant of $R(t)$ with respect to p_i . Then the greatest common divisor of these n determinants is the Alexander polynomial of virtual knot K .

5.3.2. *Contracted Gauss diagram and contracted new formula.* For virtual knots, there may be arrows with both contiguous starts and contiguous tips in the Gauss diagram \mathbb{G} . Merge all such adjacent arrows together and label each merged arrow c_i with the number of the original arrows, denoted ω_i , then we call it *contracted Gauss diagram*, denoted \mathbb{G}^ω . For base point p_n , we define a matrix $\mathbf{R}(t)$ from \mathbb{G}^ω as follows.

$$\mathbf{R}_{ii}(t) = \begin{cases} -1, & \text{if } \text{sgn}P_i = \text{sgn}c_i; \\ -t, & \text{if } \text{sgn}P_i = -\text{sgn}c_i. \end{cases}$$

$$\mathbf{R}_{ji}(t) = \begin{cases} t^{\omega_i} - 1, & \text{if } c_{j0} \in P_i \text{ and } \text{sgn}P_i = \text{sgn}c_j; \\ 1 - t^{\omega_i}, & \text{if } c_{j0} \in P_i \text{ and } \text{sgn}P_i = -\text{sgn}c_j; \\ 0, & \text{if } c_{j0} \notin P_i. \end{cases} \quad \forall j \neq i,$$

An argument similar to the one used for ribbon graph shows that $|R(t)| = \pm|\mathbf{R}(t)|$. Again, the Alexander polynomial of virtual knot K is the greatest common divisor of the determinants by taking base point in the interior of all the different over-passing arcs on \mathbb{G}^ω .

Corollary 5.3.1. *The Alexander polynomial of a virtual knot depends only on contracted Gauss diagram.*

This new formula (5.3.1) can sometimes simplify the calculation of Alexander polynomial considerably.

Example 5.3.2.

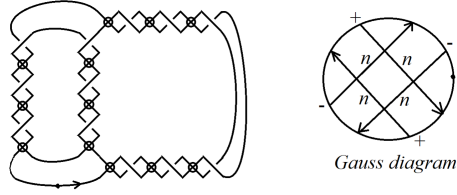
$$\mathbf{R}(t) = \begin{pmatrix} -t & 0 & 0 & 0 \\ 1 - t^n & -1 & 1 - t^n & 0 \\ t^n - 1 & 1 - t^n & -1 & t^n - 1 \\ 0 & t^n - 1 & 0 & -t \end{pmatrix},$$

thus $|\mathbf{R}(t)| \doteq - (t^n - 1)^3 + t^{n+1}(t^n - 2)$. By symmetry of the knot, we can derive $\Delta_{K_n}(t) \doteq - (t^n - 1)^3 + t^{n+1}(t^n - 2)$.

:

6. QUESTIONS AND A GENERALIZATION

6.1. **Questions.** We propose two questions, which may be not quite difficult, but of independent interests.

FIGURE 33. A series of virtual knots K_n . Here $n = 3$.

6.1.1. *Geography of half Alexander polynomials for symmetric unions.* Symmetric unions were first introduced by Kinoshita and Terasaka [9] and generalized by Lamm in [11]. Each symmetric union has a canonical ribbon R by adding twists to the canonical ribbon of $\mathbb{K}\# - \overline{\mathbb{K}}$, where \mathbb{K} is its partial knot. Lamm [11] conjectured in 2000 that every knot is a symmetric union, which is still open [12].

For a symmetric union, the ribbon diagram of R is the middle of Fig. 27 with several small triangles reversed, which corresponds to changing several signs in the Gauss diagram of \mathbb{K} , and to changing the directions of several edges in the ribbon tree. Then we can use $W^*(t)$ in Theorem 4.5.2, or equivalently $(n-1) \times (n-1)$ minor of W from Fig. 1 with signs of some crossings changed, to compute $A_R(t)$.

For any knot, $(n-1) \times (n-1)$ minor of W gives its Alexander polynomial, which is palindromic. We ask

Question 6.1.1. For any $f(t) \in \mathbb{Z}[t]$ with $f(1) = \pm 1$, is there is a canonical ribbon of symmetric union so that the half Alexander polynomial $A_R(t) \doteq f(t)$?

If the answer was false, one might easily get infinitely many counterexamples to Lamm's conjecture.

6.1.2. *Fusion number.* The number g in the definition of ribbon diagram is called *ribbon number* of the ribbon. However, the most researched ribbon knot invariant is *fusion number*, which is the minimal number of fusions among all the ribbons for it. For a ribbon, fusion number can be much smaller than ribbon number. As ribbon graph is a reasonable notation to represent a ribbon, we ask

Question 6.1.2. How to know the fusion number of a ribbon from its ribbon graph?

6.2. **A generalization.** Consider a split union of knots. To be specific, let $\Omega_1, \dots, \Omega_n$ be disjoint balls in S^3 and K_i be a knot (maybe unknot) in Ω_i for $i = 1, \dots, n$. Let B_1, \dots, B_{n-1} be disjoint bands each connecting two knots with two arcs in the boundary so that $\cup_{i=1}^n K_i \cup \cup_{i=1}^{n-1} \partial B_i - \text{int}(\cup_{i=1}^n K_i \cap \cup_{i=1}^{n-1} \partial B_i)$ is a knot, denoted K . See Fig.33 for an example. We give a formula for Alexander polynomial of K .

Suppose $\cup_{i=1}^{n-1} \partial B_i$ intersects $\Omega_1, \dots, \Omega_n$ transversely in arcs. Let b_i be the core arc of B_i connecting different knot components for $i = 1, \dots, n-1$, oriented temporarily. Denote the components of $b_i \cap \cup_{j=1}^n \Omega_j$ in order along b_i by $b_{i0}, b_{i1}, \dots, b_{i, x_i}$. For each proper arc component $b_{ik} \subset \Omega_j$, there is a well-defined linking number $lk(b_{ik}, K_j)$. Denote the components of $b_i - \cup_{j=1}^n \Omega_j$ in order along b_i by $v_{i1}, \dots, v_{i, x_i}$. We now define a *contracted ribbon graph* (T^ω, S) , where T^ω is a weighted directed tree and S is a map from its edges to its vertices, as follows.

- *Tree T^ω :* The vertex set consists of vertex V_i corresponding to K_i for $i = 1, \dots, n$ and vertices $v_{i1}, \dots, v_{i, x_i}$ for each $i = 1, \dots, n-1$. Each b_{ik} gives an edge

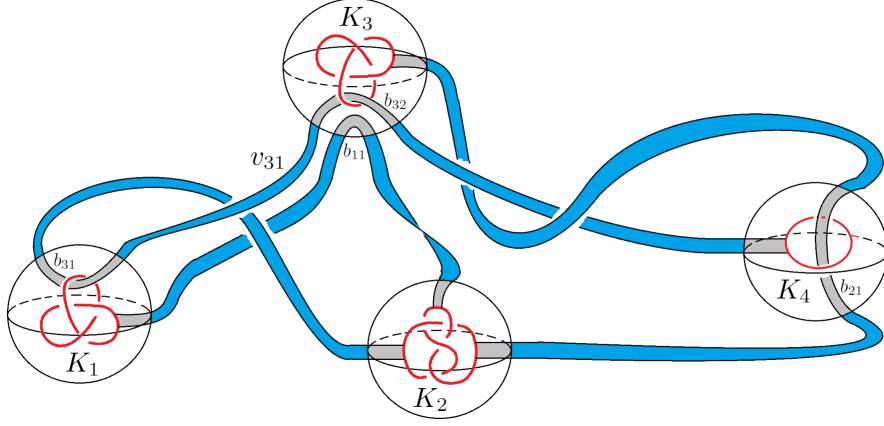
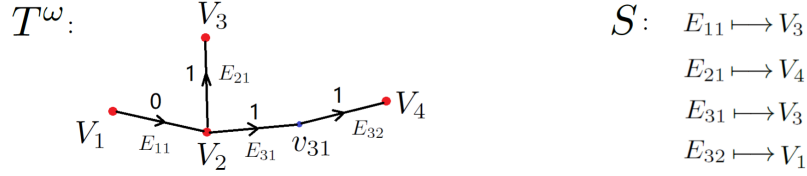
FIGURE 34. An example of $\cup_{i=1}^n K_i \cup \cup_{i=1}^{n-1} B_i$.

FIGURE 35. Contracted ribbon graph.

E_{ik} incident to the two vertices containing the endpoints of b_{ik} . Assume $b_{ik} \subset \Omega_j$, then the direction of E_{ik} is from $v_{i,k-1}$ to v_{ik} if $lk(b_{ik}, K_j) > 0$ and opposite if otherwise. The weight of E_{ik} , denoted ω_{ik} , is $|lk(b_{ik}, K_j)|$. Contract each edge E_{i0} and each edge E_{i,x_i} .

- Singularity map S : $S(E_{ik}) = V_j$ if and only if $b_{ik} \subset \Omega_j$.

For example, Fig. 34 is the contracted ribbon graph for Fig.33. Then we define a matrix $(\mathbf{R}_{ij}(t))$ from (T^ω, S) according to (5.3.1) and the paragraph before it.

Theorem 6.2.1. *With the above notations, the Conway-normalized Alexander polynomial of K is*

$$\Delta_K(t) = |\mathbf{R}_{ij}(t)| |\mathbf{R}_{ij}(t^{-1})| \Delta_{K_1}(t) \cdots \Delta_{K_n}(t).$$

Especially, Alexander polynomials of K is determined by the Alexander polynomials of K_1, \dots, K_n and the contracted ribbon graph.

Rather than give a detailed proof we outline it. We will prove a more general result in detail including this theorem as a special case in [1].

Proof. First, let $F_i \subset \Omega_i$ be a Seifert surface for K_i so that $\cup_{i=1}^n F_i \cup \cup_{i=1}^{n-1} B_i$ is a immersed surface with only ribbon singularities. Suppose the subband of B_i corresponding to $b_{ik} \subset \Omega_j$ has ribbon arcs $\beta_{ik1}, \dots, \beta_{ik,y_{ik}}$. Desingularize the immersed surface into a Seifert surface for K , denoted F_K , as in 3.3.1.

Second, let $h_{i1}, \dots, h_{i,z(i)}$ be a basis of $H_1(F_i)$. Let $e_{ik,l}$ be a small circle encircling $\beta_{ik,l}$. Choose $f_{ik,l}$ to be the path on the immersed surface and $f_{ik,l}$ be the simple closed curve on F_K as in 3.3.2.

Then all of e_{\dots} , all of f_{\dots} and $h_{11}, \dots, h_{1,z(1)}, \dots, h_{n1}, \dots, h_{n,z(n)}$ form a basis of $H_1(F_K)$. The Seifert matrix of F_K has the form

$$A = \begin{pmatrix} O & P & O & & & \\ Q & L & * & & & \\ & & A_1 & & & \\ O & * & & \ddots & & \\ & & & & & A_n \end{pmatrix},$$

where A_i is a Seifert matrix for K_i .

Therefore

$$\Delta(t) = |t^{\frac{1}{2}}A - t^{-\frac{1}{2}}A^T| = |tP - Q^T||t^{-1}P^T - Q|\Delta_{K_1}(t) \cdots \Delta_{K_n}(t).$$

We can obtain P, Q exactly as in 3.3.3 to get formula (3.2.2).

Finally, preceding exactly as in 4.4, we have $|\mathbf{R}_{ij}(t)| = |tP - Q^T|$. \square

Acknowledgement: I am grateful to Jianhua Tu for his direction in graph theory and his help in writing Subsection 3.1 and 3.2. I gratefully acknowledges Professor Tetsuya Ito for his guidance in writing this paper. I thank Juhasz, Kauffman and Ogasa for their patience in discussing with me when I found there was a very implicit connection between our Theorem 5.2.1 and their construction of twins Alexander polynomial in [7].

REFERENCES

- [1] S. Bai, *Alexander polynomials from compressing surfaces with double singularities*, in preparation.
- [2] S. Chmutov, M. Khoury, A. Rossi, *Polyak-Viro formulas for coefficients of the Conway polynomial*, J. Knot Theory Ramifications 18 (6) (2009), pp. 773-783.
- [3] M. Eisermann, C Lamm, *Equivalence of symmetric union diagrams*, J. Knot Theory Ramifications 16, 879 (2007) 879898.
- [4] R. H. Fox, J. W. Milnor, *Singularities of 2-spheres in 4-space and equivalence of knots*, unpublished.
- [5] S. Friedl, M. Powell *A Calculation of Blanchfield Pairings of 3-Manifolds and Knots*, Moscow Mathematical Journal 17(1) (2017):59-77.
- [6] M. Goussarov, M. Polyak and O. Viro, *Finite type invariants of classical and virtual knots*, Topology 39 (2000) 1045-1068.
- [7] A. Juhasz, L. H. Kauffman, E. Ogasa *New invariants for virtual knots via spanning surfaces*, arXiv:2207.08129.
- [8] K. Kishimoto, T. Shibuya, T. Tsukamoto, T. Ishikawa *Alexander polynomials of simpleribbon knots*, Osaka J. Math.58 (2021), 41-57.
- [9] S. Kinoshita and H. Terasaka. *On unions of knots*, Osaka Math. J., 9:131-153, 1957.
- [10] L. H. Kauffman *On knots*, Princeton Univ. Press, Princeton 1987.
- [11] C. Lamm *Symmetric Unions and Ribbon Knots*, Osaka J. Math. 37 (2000), 537-550.
- [12] C. Lamm *The Search for Nonsymmetric Ribbon Knots*, Experimental Mathematics, 30:3, 349-363.
- [13] W. B. Raymond Lickorish *An introduction to knot theory*, Graduate Texts in Mathematics, vol. 175, Springer-Verlag, New York, 1997. MR 1472978.
- [14] C. Livingston. *A survey of classical knot concordance*, In Handbook of knot theory, pages 319-347. Elsevier B. V., Amsterdam, 2005.
- [15] H. Terasaka. *On null-equivalent knots*, Osaka Math. J. 11 (1959), 95-113.

Email address: barry011000@outlook.com